Article

Effect of Temperature, Wettability and Relative Permeability on Oil Recovery from Oil-wet Chalk

Aly A. Hamouda* and Omid Karoussi

Department of Petroleum Engineering, University of Stavanger, 4036 Stavanger, Norway

* Author to whom correspondence should be addressed; E-mail: aly.hamouda@uis.no

Abstract: It is customary, for convenience, to use relative permeability data produced at room temperature. This paper shows that this practice underestimates oil recovery rates and ultimate recovery from chalk rocks for high temperature reservoirs. Above a certain temperature (80°C in this work) a reduction of oil recovery was observed. The reduction in oil recovery is reflected by the shift of relative permeability data towards more oil-wet at high temperature (tested here 130°C). However, both IFT and contact angle measurements indicate an increase in water wetness as temperature increases, which contradict the results obtained by relative permeability experiments. This phenomenon may be explained based on the total interaction potential, which basically consists of van der Waals attractive and short-range Born repulsive and double layer electrostatic forces. The fluid/rock interactions is shown to be dominated by the repulsive forces above 80°C, hence increase fine detachment enhancing oil trapping. In other words the indicated oil wetness by relative permeability is misleading.

Keywords: Temperature, Relative Permeability, Oil Recovery, Wettability (Contact angle), Interfacial tension (IFT), Fluid/rock interaction

1. Introduction

Improving oil recovery is recognized as the major target and challenge at the different stages of an oil field development. Among several methods in oil recovery, thermal recovery has been used to increase the mobility of oil specifically in heavy crude oil reservoirs. Babadagli [1-2] compared the

recovery rate of different types of crude oil in naturally fractured reservoirs. He reported that the reduction in oil viscosity due to the high temperature fluid injection (hot water) accelerates the imbibition recovery rate. Babadagli and Al-Bemani [3] investigated the effect of steam injection on oil recovery of carbonate reservoir rock containing heavy oil. They showed that thermal expansion mechanism predominantly controls the recovery.

In addition to the temperature effect on oil mobility, temperature also alters the wettability of oil-wet rock to more water-wet, which contributes to enhance oil recovery. Rao [4] stated that although reduction in oil viscosity may be the main purpose of thermal recovery, the thermal energy imposed on the system, introduces changes not only in fluid properties and fluid-fluid interactions but also in rock-fluids interaction characterized by wettability. Tang and Morrow [5-6] reported a transition toward more water-wet behavior in Berea sandstone, when temperature increased to 75°C under water imbibition/flooding process. Al-Hadhrami and Blunt [7] in a field case study showed that at a transition temperature chalky limestone rock would undergo through a wettability reversal process from oil-wet to water-wet with temperature. Schembre *et al.* [8] also correlated the improvement in oil recovery from diatomaceous rock to the alteration of wettability at elevated temperature by renewal of surfaces.

Hamouda and colleagues [9-16] in a series of works dealing with chalk/water/oil interactions, revealed that increasing temperature in oil/water/solid rock system, improves the water wetness of oil-wet chalk, and they reported an increase in oil recovery under a spontaneous imbibition scheme, reduction in the measured contact angles and IFT. They also presented a series of calculations on the wettability alteration mechanism at elevated temperatures taking into account the fluid/rock interaction forces and disjoining pressure [14].

In this work, the effects of temperature and relative permeability on oil recovery are investigated. An experimental and a simple model of reservoir performance at elevated temperature are addressed in this paper as an attempt to explain the possible cause of adverse effect of temperature on reservoir performance.

2. Results and Discussion

2.1. Simulation of oil recovery: temperature effect

In this section, the effect of temperature on oil recovery is modeled using the Eclipse 100 simulator software, where except for the injected water temperature, the input model characteristics such as PVT, relative and absolute permeability data are kept constant for simulation runs. The thermal option is activated following the recommendations in reference [17]. Water at 6 different temperatures: 26.7°C (80°F), 40°C (104°F), 57.2°C (135°F), 70°C (158°F), 90°C (194°F) and 100°C (212°F) are injected into the reservoir with an initial temperature of 57.2°C (135°F).

Experimental oil/water relative permeabilities at room temperature (23°C) are used in order to isolate the effect of the temperature alone on oil recovery. As shown in Figure 1, the ultimate oil recovery factor (RF) increases to about 12.5% from ~0.35 to ~0.4, as injecting water temperature increased from 26.7°C (80°F) to 100°C (212°F). The increase of the oil recovery may be due to the increase of the oil mobility and fluid expansion. Oil recovery by spontaneous imbibition shows an

increasing trend with temperature (Tang and Morrow [5-6], Schembre *et al.* [8], Hamouda and Rezaei Gomari [9], and Karoussi and Hamouda [14]). Wettability alteration is not a direct option in Eclipse simulator; Delshad *et al.* [18] adapted a chemical flooding simulator to include wettability alteration process. Relative permeability data for 4 temperatures are used here as indirect indication of wettability alteration in the later runs.

Figure 1. Simulated oil recovery factor (RF) of injecting water at different temperature from 26.7°C (80°F) to 100°C (212°F). Room temperature relative permeability data are used in this case. Reservoir Temperature is taken to be 57.2°C (135°F). The higher the temperature of the injected water, the higher recovery factor is.
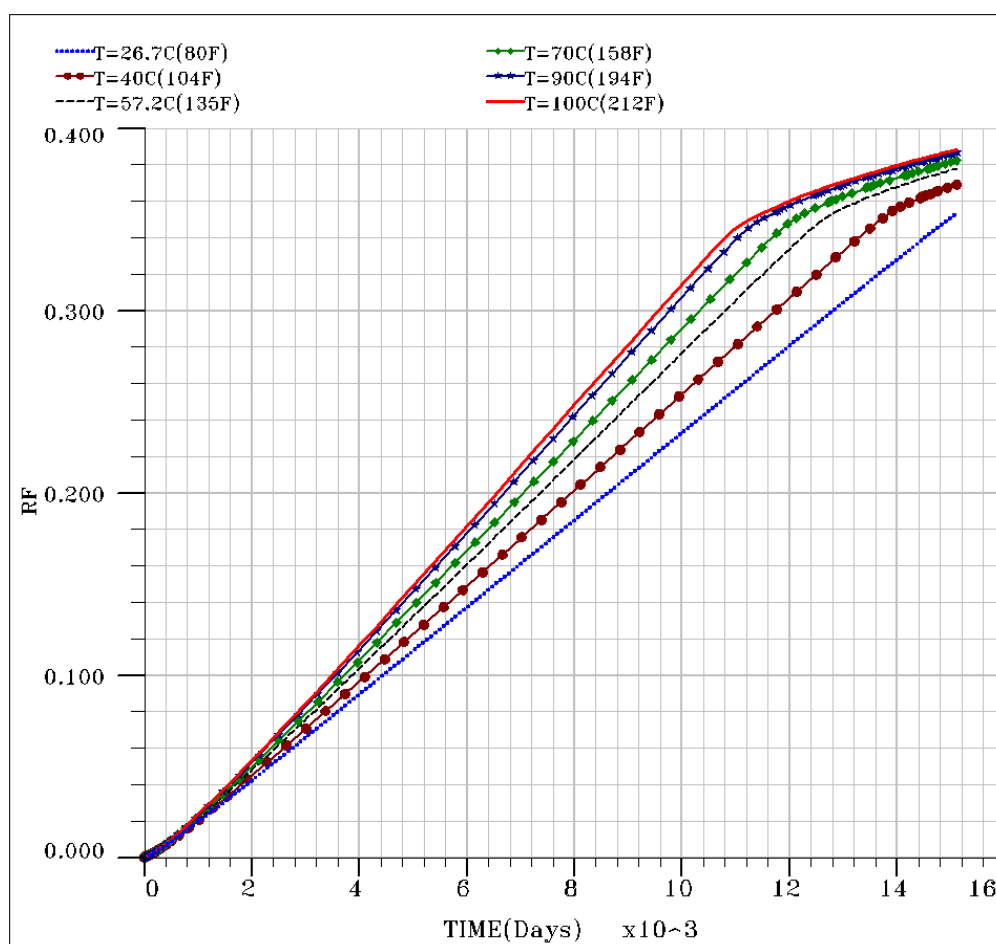

2.2. Oil recovery sensitivity to different temperature relative permeability data

In previous work [16] Hamouda *et al.* showed that the intersection of oil/water relative permeability of modified chalk is shifted toward the right side, indicating more water-wet behavior as the temperature increases up to 80°C. The relative permeability data are presented in Figure 2. Experimental data at high temperature of 130°C shows a shift of oil and water relative permeabilities intersect toward left (indicating more oil-wet behavior).

In order to investigate the effect of relative permeabilities at elevated temperatures on oil recovery, relative permeability data for four different temperatures (23, 50, 80 and 130°C as shown in Figure 2) are input into the reservoir simulator while oil/water PVT properties, water injection rate under constant bottom hole pressure, reservoir model geometry, production time are kept constant. Figure 3 shows a higher oil recovery of about 48% and the lowest one of about 26%, corresponding to relative permeability data at the temperatures of 80 and 130°C, respectively.

Figure 2. Effect of temperature on relative permeability for oil-wet chalk cores with 0.005MSA dissolved in decane. (From Hamouda *et al.* [16]).
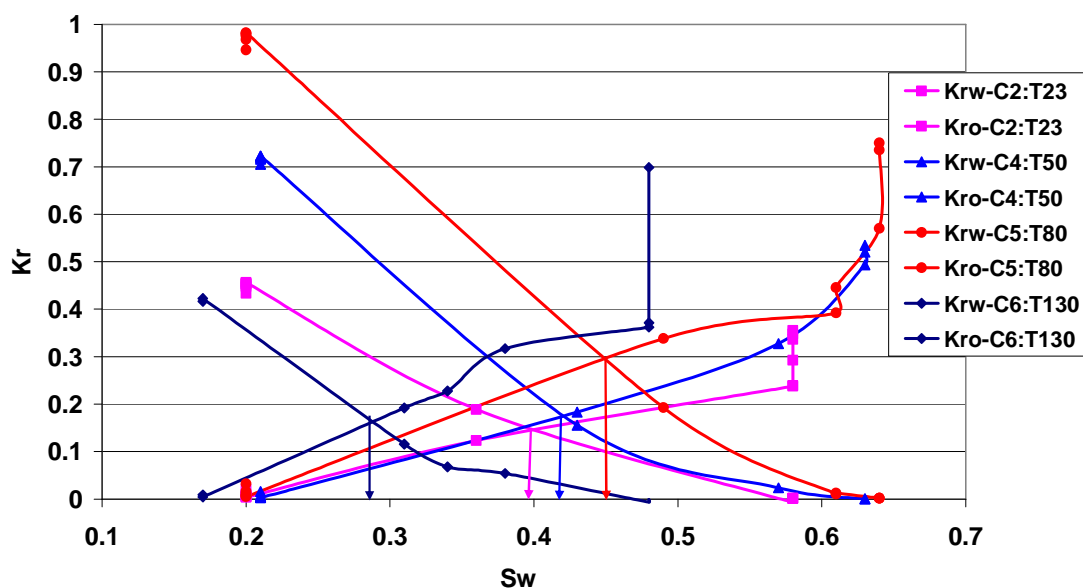

Three main observations may be deduced from Figure 3. A maximum recovery of 48% is obtained, when 80°C relative permeability data is used, while the lowest recovery is obtained, when relative permeability data is used at 130°C. So, the recovery increased when the temperature reached 80°C and then declined at 130°C. There are no surprises from the simulated data, since the results reflect the obtained experimental relative permeability data. In quantitative sense of oil recovery, an increase of S_w (at the intersect between k_{ro} and k_{rw}) by 7% (from 23 to 50°C) and by 16% (from 50 to 80°C) corresponds to an increase of ultimate oil recovery and about 25%, respectively. A reduction of recovery of about 22% is obtained when the temperature was raised from 80 to 130°C. This corresponds to a reduction of S_w to 20%. The small difference in the recovery rates and ultimate RF level obtained for relative permeability data of 23 and 50°C may be due to that the simulated reservoir temperature is at about 57.2°C (135°F), hence the oil mobilities for 23 and 50°C cases become close as the injection proceeds.

The second observation is that at higher temperature (80°C), in this work, faster and higher oil recovery is obtained, which may reflect both oil mobility and wettability alteration by temperature, as indicated by intersection between k_{ro} and k_{rw}, that increased from about 7 to 16%, when temperatures increased from 23 to 50°C and from 50 to 80°C, respectively as shown in Figure 2.

The third observation is that, the point of time at which the recovery rate is reduced is reached faster at higher temperatures than that at lower temperatures. It is interesting to observe (Figure 3) that both 80 and 130°C have reached that point at almost the same time, in spite of the lower rate and recovery in case of 130°C.

In general from this work and the work done by Nakornthap and Evans [19], it may be concluded that use of room temperature relative permeability underestimates the oil recovery rate and ultimate recovery. It may, also, be concluded that not only the injected fluid temperature that affect the recovery rate and ultimate recovered oil but also temperature difference between the injected fluid and the reservoir temperature. The above simulation and discussion does not address the wettability change to more oil-wet, hence reduced oil recovery at 130°C.

Figure 3. Simulated oil recovery factor as a function of relative permeability at 23, 50, 80 and 130°C.
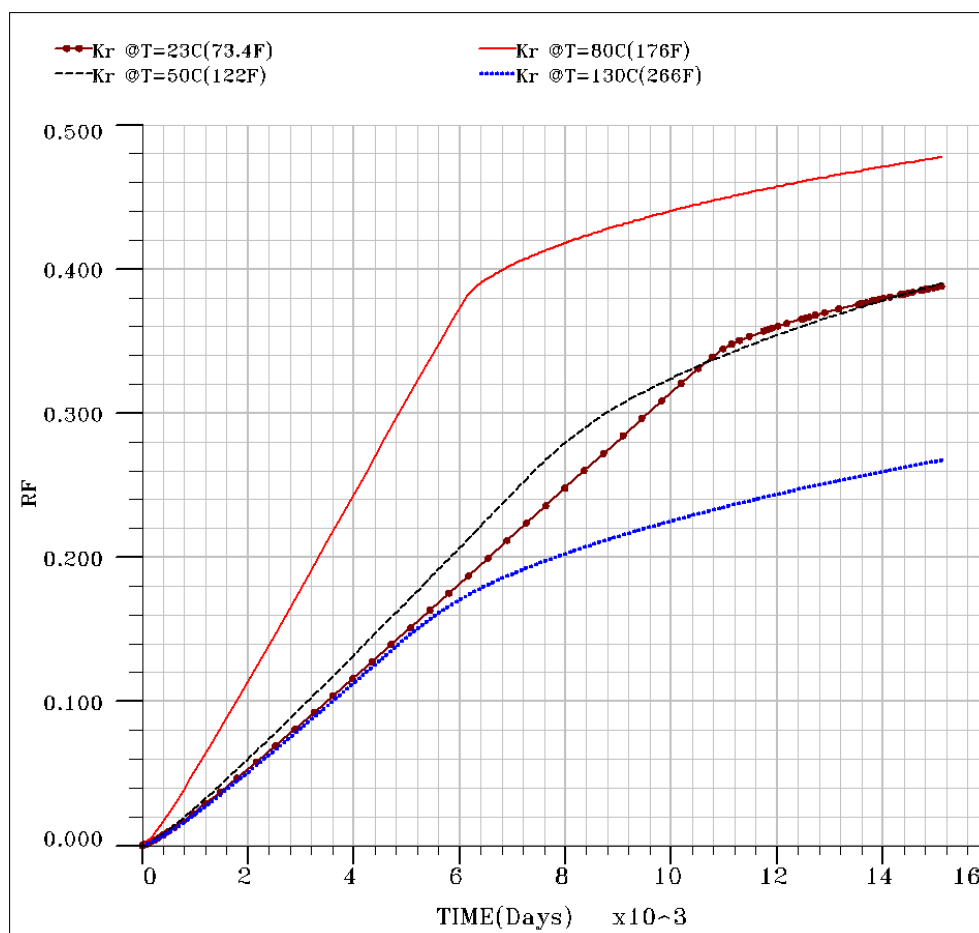
In order to approximate the relative permeability as a function of temperature, Nakornthap and Evans' equations [19] (i.e. equations 3 and 4) are used. It must be stated here that it is assumed that fluids are incompressible; the changes in porosity and rock bulk volume are independent on temperature.

$$\frac{dk_{rw}}{dT} = -\left(\frac{2+3\lambda}{\lambda}\right) \times \frac{(S_w - S_{wir})^{2(1+\lambda)/\lambda}(1-S_w)}{(1-S_{wir})^{2(1+2\lambda)/\lambda}}\left(\frac{dS_{wir}}{dT}\right) \tag{1}$$

$$\frac{dk_{ro}}{dT} = \left\{\left(\frac{2+\lambda}{\lambda}\right)\frac{(S_w - S_{wir})^{2/\lambda}(1-S_w)^3}{(1-S_{wir})^{2(1+2\lambda)/\lambda}} + 2\left[1-\left(\frac{(S_w-S_{wir})}{(1-S_{wir})}\right)^{(2+\lambda)/\lambda}\right]\frac{(1-S_w)^2}{(1-S_{wir})^3}\right\}\left(\frac{dS_{wir}}{dT}\right) \tag{2}$$

$$k_{rw} = \left(\frac{S_w - S_{wir}}{1-S_{wir}}\right)^{(2+3\lambda)/\lambda} \tag{3}$$

$$k_{ro} = \left[1-\left(\frac{S_w - S_{wir}}{1-S_{wir}}\right)\right]^2 \times \left[1-\left(\frac{S_w - S_{wir}}{1-S_{wir}}\right)^{(2+\lambda)/\lambda}\right] \tag{4}$$

where, λ is pore size distribution index. The corresponding irreducible water saturation (S_{wir}) and λ values at each temperature are given in Table 1. The generated oil/water relative permeabilities are shown in Figure 4.

**Table 1.** S_{wir} and λ for experimental relative permeability data.

Temperature (°C)	S_{wir}[1] (%)	λ[1]
23	20	6.62
50	21	5.67
80	20	9.835
130	17	4.241

(1) Hamouda *et al.* [16]

At first glance the trends of the approximated relative permeabilities as a function of temperature shown in Figure 4, may seem to contradict equations 1 and 2, especially for the case where the temperatures increased from 80 to 130°C.

In equations 1 and 2, if one assumes that in general S_{wir}, increases with temperature, a positive value of dS_{wir}/dT leads to a decrease and increase of the water and oil relative permeabilities as a function of temperature (dk_{rw}/dT and dk_{ro}/dT), respectively. This agrees with the obtained results, where the temperature increase from 23 to 50°C is associated with the increase of S_{wir} from 0.2 to 0.21, respectively. The agreement with the predicted trend is also due to the close values of λ in both cases. At the two other temperatures, 80 and 130°C, S_{wir} from the experiments are 0.2 and 0.17, which are equal to and less than that obtained at 23°C, respectively. However, due to the large difference in the obtained λ, the predicted trend with temperature deviated. In other words, the dependence of k_{ro} and k_{rw} trend with temperature is governed not only by S_{wir}, but also λ, as shown by the equations. Nakornthap and Evans [19] used a fixed value of 2 for λ in their analysis.

Figure 4. Calculated relative permeability data using equation 3 and 4. S_{wir} and λ are taken from experimental relative permeability data.
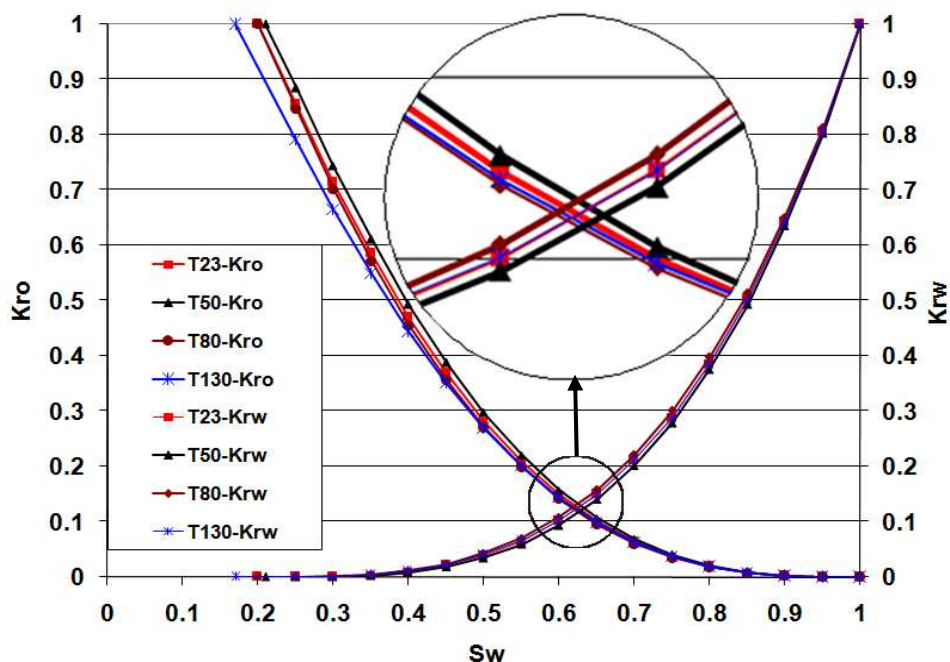

Again, no explanation is made so far to the observed increase of oil-wet status of the chalk with temperature. In our experimental work, particle production was observed from the chalk during relative permeability flooding experiments with distilled water and at 130°C. Total interaction potential for a water/oil/chalk (calcite) system was addressed earlier by Karoussi and Hamouda [14]. The findings are that the total interaction potential (consisting of van der Waals attractive, short-range Born repulsive and double layer electrostatic forces) becomes more repulsive in nature between oil-wet calcite particles and calcite wall surface in distilled water medium. The computed total interaction potentials were done previously up to 100°C; in this study the computation is extended to include 130°C. The calculated total interaction potentials for two different sizes of calcite particles (1 and 4 µm) are shown in Figure 5. Schramm *et al.* [20] and Pierre *et al.* [21] reported a value of <5 and 2µm for calcite particle size, respectively.

The positive values of ~75x10^{-18} and ~325x10^{-18} J, indicate possible detachment at temperature of 130°C for 1 and 4 µm particle size, respectively. The detachment of particle and fines migration may cause change in pore geometry of rock, consequently permeability reduction.

The investigation of the increase of the oil wetness of the chalk continued from two different angles, namely IFT and contact angle measurements, which are addressed in the next two sections.

Figure 5. Estimated interaction potential for modified calcite surfaces (0.005M SA in *n*-decane) for water/oil/chalk (calcite) for two different particle sizes 1 and 4 µm.
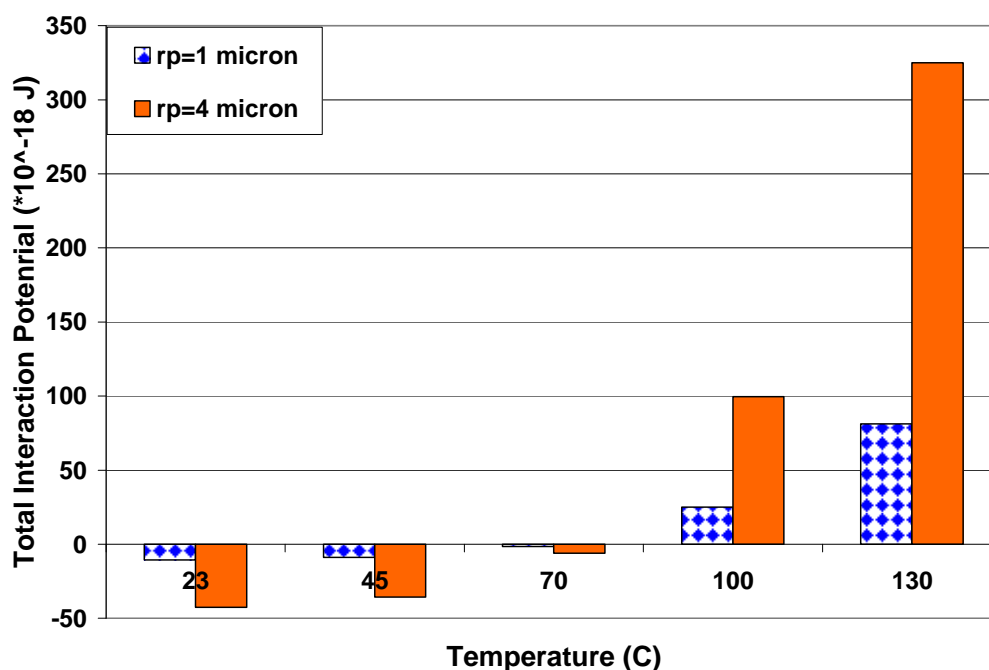
2.3. Interfacial Tension (IFT)

Interfacial tension measurements are done to confirm the effect of the temperature on the interfacial activity. Indeed interfacial tension experiments show the expected decreasing trend (form 40.1 at 28°C to 35.7 mN/m at 70°C) for 0.005M SA in *n*-decane/water system as shown in Figure 6. Hamouda and Rezaei Gomari [9] also reported a similar trend for 0.01M SA in *n*-decane/water system. The IFT measurements are performed here with 0.005M SA in n-decane/water containing 0.1M concentration of sodium sulfate or magnesium chloride, to examine the trend and the effect of these ions in salt waters. IFT in presence of magnesium ions is shown to be lower than that in presence of sulfate ions or distilled water, where 32, 34.9 and 40.1 mN/m at 28°C are measured for 0.1M $MgCl_2$, 0.1M Na_2SO_4 and distilled water, respectively. Magnesium ions also showed the lowest measured IFT for all tested temperatures. The highest interfacial activity in presence of magnesium chloride, once more demonstrate the influential role of magnesium ions in oil/water/chalk interactions that have been previously investigated with several macroscopic and microscopic approaches done by Hamouda and colleagues [10-16].

Amaefule and Handy [22] and Kumar *et al.* [23] studied the effect of IFT and IFT/temperature on oil-water relative permeability, respectively. In their investigation, they used capillary number (N_c) to relate relative permeability behavior and IFT. The equations used are general and modified definition of N_c:

$$N_c = \frac{\mu_w v}{\sigma}$$

(5)

and,

$$N_c = \frac{\mu_w v}{\sigma} \times (\frac{T}{T_b}) \times (\frac{\mu_w}{\mu_o})^{0.4} \qquad (6)$$

where, μ is viscosity; v is velocity; σ is IFT; T and T_b are temperature and room temperature, respectively. The subscripts w and o denotes for water and oil, respectively. Amaefule and Handy [22] stated that the higher N_c is required to initiate mobilization of oil. The corresponding calculated capillary numbers to the studied relative permeabilities, as shown in Figure 1, are given in Table 2 using equations 5 and 6. The calculation done by Equation 5, shows a decreasing trend for N_c, (from $N_c=3.8 \times 10^{-7}$ at 23°C to 1.75×10^{-7} at 80°C). This is in contrast to the experimental results of the relative permeabilities up to 80°C and the obtained decreasing trend of IFT with temperature.

Figure 6. Comparison between the average measured IFTs of 0.005M SA dissolved in *n*-decane and distilled water (DW), 0.1M Na_2SO_4 and 0.1M $MgCl_2$ as a function of temperature. The error bars represents, the standard deviation of the experimental data varies between ±0.1to 0.4 mN/m.
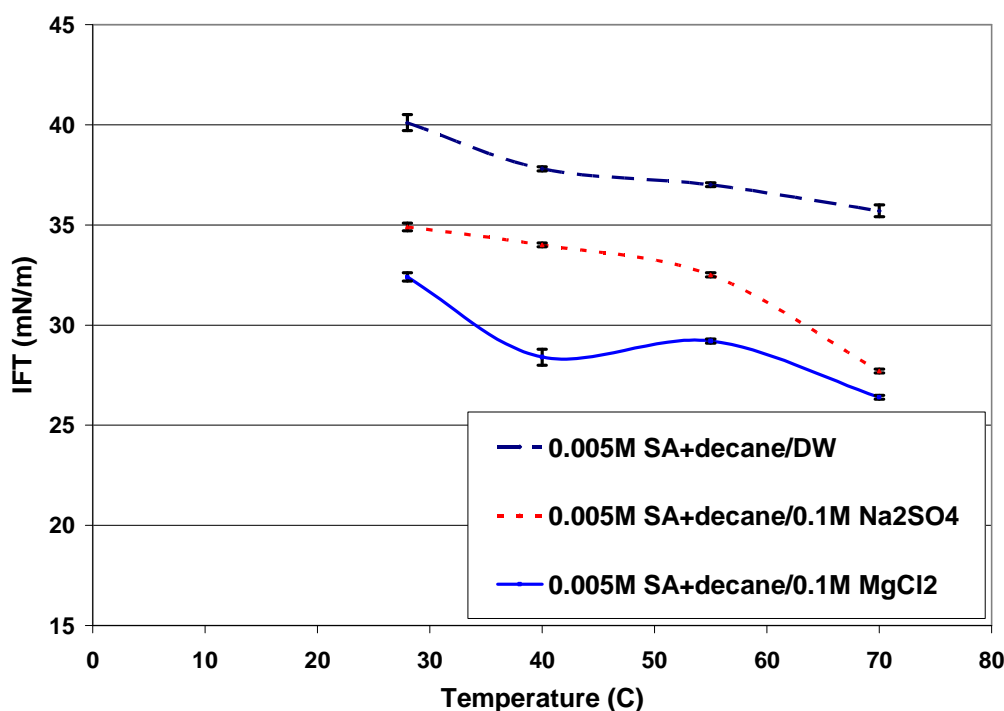
The modified capillary number equation (Equation 6), on the other hand, shows an increasing trend of N_c as temperature increases, $N_c=3.93 \times 10^{-7}$ at 23°C to 5.41×10^{-7} at 80°C, which agrees with the results presented by Kumar *et al.* [23]. The increasing trend of N_c may explain the improvement of relative permeability up to 80°C, where a reduction in S_{or} is observed experimentally. As can be seen, in spite of reduction in IFT and viscosity at 130°C, a decrease in N_c is obtained; (reduction from 5.41×10^{-7} at 80°C to 4.31×10^{-7} at 130°C), which may provide a qualitative explanation to the more oil-wet behavior from the relative permeability experimental data at 130°C.

Table 2. Capillary number determination as a function of temperature, IFT and viscosity.

T °C	S_{wir}	S_{or}	μ_w N.s/m^2	μ_o N.s/m^2	σ_{ow} mN/m	$N_c = \dfrac{\mu_w v}{\sigma}$	$N_c = \dfrac{\mu_w v}{\sigma} \times (\dfrac{T}{T_b}) \times (\dfrac{\mu_w}{\mu_o})^{0.4}$
23	0.2	0.42	0.00100	0.00092	40.1	3.8×10^{-7}	3.93×10^{-7}
50	0.21	0.37	0.00055	0.00061	37	2.28×10^{-7}	4.74×10^{-7}
80	0.2	0.36	0.00036	0.00047	34.537	1.75×10^{-7}	5.41×10^{-7}
130	0.17	0.52	0.00018	0.00029	29.637	9.19×10^{-8}	4.31×10^{-7}

2.4. Contact Angle

The measured advancing and receding contact angles as a function of temperature for modified calcite surfaces with 0.005M SA dissolved in decane are shown in Figure 7. Contact angle decreases with temperature; indicating that the calcite surface is becoming more water-wet as a function of temperature as shown in Figure 7.

Figure 7. Advancing and receding contact angles as a function of temperature in a water medium for modified calcite surfaces with 0.005M SA dissolved in *n*-decane.
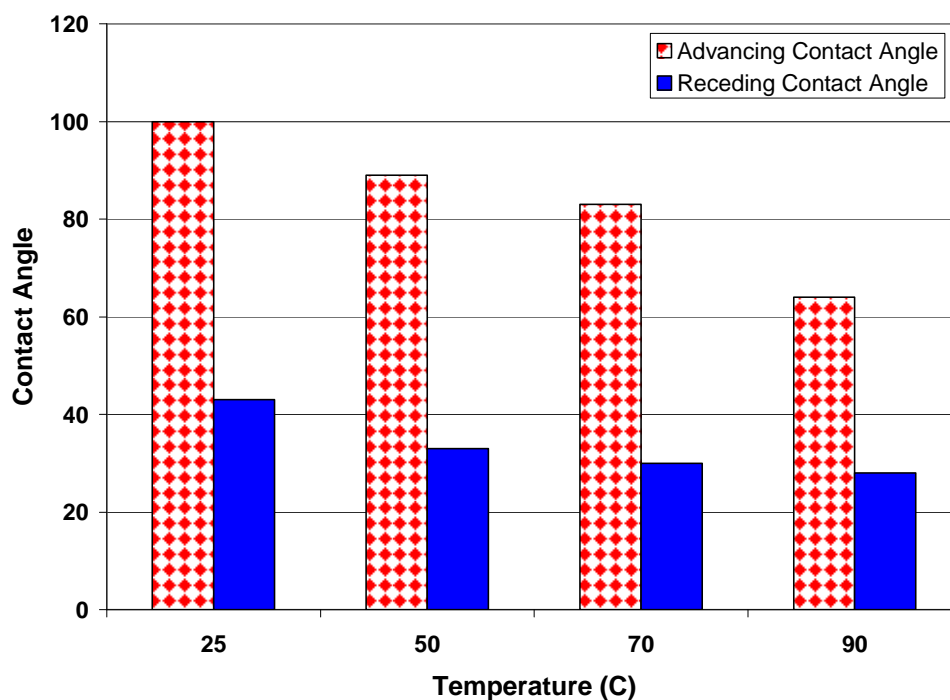
2.5. An Approach for estimation/verification of contact angle

Bahramian and Danesh [24] reported an approach to predict solid-water-hydrocarbon contact angle as well as surface/interfacial tension on the basis of mutual solubility of two components/phases. The

following equations and given data in Table 3, are applied in this study for SA/*n*-decane/water system to compare the predicted contact angle with the measured values. It was assumed that stearic acid completely adsorbs on the calcite surface; hence, SA is considered as the solid phase rather than calcite.

$$\sigma^{12} = \frac{1}{2} \times \frac{A}{a_{12}} \tag{7}$$

$$A = RT \times \frac{\ln(X_1^2 / X_1^1)}{(X_2^1)^2 - (X_2^2)^2} \tag{8}$$

$$a_i = V^{2/3} N^{1/3} \tag{9}$$

where, σ^{12} is the interfacial tension between component 1 and 2; R is the ideal gas constant; T is temperature in (K); a_{12} is the average partial molar surface area; a_i is the partial molar surface area of component i; V is molar volume and N is Avogadro's number. X_i^j is the mole fraction of component "i" in rich phase of component "j".

Table 3. Applied mutual solubility data in water/SA/decane system for IFT calculations.

Mutual Solubility data	
Solubility of water in *n*-C10 @ 25°C	0.072 g water/1000 g C10
Solubility of *n*-C10 in water @ 25°C	1.98E-6 g C10/100 g water
SA concentration in decane (Table 4a)	0.005 M
SA concentration in decane (Table 4b)	0.01 M
Decane fraction in SA	~0
Water fraction in SA	~0
SA solubility in water	0.034 g SA/100 g water

For SA/*n*-decane/water system, the mutual interfacial tension between each phase is determined using Equation 7. The calculated interfacial tension values and the corresponding contact angle are compared as shown in Tables 4a and 4b for 0.005 and 0.01M concentrations of SA, respectively.

Table 4a. Calculated IFT and Contact angle for water/0.005M SA/decane system.

$\sigma_{water/C10}$ (mN/m)	$\sigma_{water/SA}$ (mN/m)	$\sigma_{0.005MSA/C10}$ (mN/m)	Θ Young eq.	Θ If $\sigma_{water/SA}$=18.05[a] (mN/m)	Θ Measured
49	58.8	25.7	47.5	99.1	90[b]

Table 4b. Calculated IFT and Contact angle for water/0.01M SA/decane system

$\sigma_{water/C10}$ (mN/m)	$\sigma_{water/SA}$ (mN/m)	$\sigma_{0.01MSA/C10}$ (mN/m)	Θ Young eq.	Θ If $\sigma_{water/SA}$=18.05[a] (mN/m)	Θ Measured
49	58.8	23.2	43.4	96.1	96[c]

a) Rezaei Gomari *et al.* [13]

b) Karoussi and Hamouda [14]

c) Rezaei Gomari *et al.* [10]

Tables 4a and 4b show the calculated contact angles using young equation, which largely differ from the measured contact angles (i.e. 47.5° compared to the measured 90° and 43.4° compared to the measured 96°, respectively).

However, when the spreading tension of water/calcite/decane system (i.e.18.05 mN/m) reported by Rezaei Gomari *et al.* [13] is used, the calculated contact angle is shown to be closer to the measured values for the two different concentrations of stearic acid (Tables 4a and 4b). It is worth mentioning that, the measured IFT for water/decane system in this study are 47 and 46.3 mN/m at 28°C, which are in agreement with the calculated value of 49 mN/m based on equation 5. Rezaei Gomari *et al.* [11] and Bahramian and Danesh [24] reported values of 45.5 and 48 mN/m for the IFT between water and *n*-decane, respectively. Bahramian and Danesh [24] correlated the calculated contact angle to the average value of advancing and receding contact angles, where in our system as shown in Figure 6, would be around 72°, which is significantly different from the calculated value of 47.5°. It should be stated that due to the lack of data and more contact angle measurement results, no generalization can be made for prediction of contact angle at this point.

Although the maximum measured IFT and contact angle was done at temperatures less than that employed during relative permeability experiments of 130°C due to the measurements limitation, the decreasing trend is in favor of increasing oil recovery, hence it may be concluded that the shift in the relative permeability at 130°C towards less S_w is mainly due to change in pore geometry of rock caused by fine detachment/migration and possible oil trapping.

An experiment is done here to further verify the above hypothesis of fine detachment/migration and possible oil trapping. Absolute permeability measurement was carried out at 23 and 130°C. Two cores were flooded by distilled water (DW) and the third one with *n*-decane. The absolute permeability was reduced by almost 50% in all cases as shown in Table 5, where the temperature increased to 130°C. This is in agreement with the statement by Nakornthap and Evans [19], that Cassé and Ramey [25], Weinbrandt *et al.* [26], and Gray *et al.* [27] found that absolute permeability decreases with temperature. Sedaee Sola *et al.* [28] reported that limestone showed a more oil-wet (as indicated by a shift of the relative permeability curves) behavior when temperature increased to 200°F (≈93°C).

Table 5. Core data and the estimated absolute permeability at 23 and 130°C.

Core#	L(cm)	D(cm)	Flooding fluid	K@ 23°C (md)	K@ 130°C (md)
A	6.15	3.75	DW	3.6	1.92
B	4.42	3.8	DW	3.57	1.88
C	4.9	3.75	*n*-decane	3.05	1.55[*]

* *n*-decane viscosity was obtained from Lee and Ellington [29]

3. Conclusions

In general it may be concluded that use of room temperature relative permeability underestimates the oil recovery rate and ultimate recovery. It may, also, be concluded that not only the injected fluid temperature affect the recovery rate and ultimate recovered oil, but also the temperature difference between injected fluid and reservoir temperature.

Above a critical temperature, an adverse effect of temperature is observed, where the relative permeabilities indicate a more oil-wet behavior. In this work, it is shown that above 80°C (tested 130°C) the intersection of the relative permeabilities is shifted toward a lower water saturation, where less oil recovery is obtained. This observation is neither supported by IFT nor contact angle as a function of temperature, as both show a decrease with temperature favoring higher oil recovery. However, this pseudo oil-wet behavior may be explained based on trapped oil due to fine detachment and migration during flooding due to total interaction potential between the fluid and the rock that becomes more repulsive at higher temperatures.

4. Experimental Section

4.1. Materials

Decane (VWR International AS, Norway) used as oil phase in this work was of 95% purity for interfacial measurement and 99% for contact angle measurements. Fluka AS (Norway) supplied stearic acid (SA, >98.5%). The aqueous phase used is either distilled water or 0.1M concentration of sodium sulfate or magnesium chloride. The calcite crystals, used in contact angle measurements, are "Island-spar" calcite from India, supplied by J. Brommeland AS (Norway).

4.2. Methods

4.2.1. Interfacial tension measurements

The interfacial tension (IFT) measurement is performed by the volume drop method, using a drop volume tensiometer (type DVT30) supplied by KRÜSS GmbH (Germany).

4.2.2. Contact angle measurements

Contact angle measurements were carried out at four different temperatures. The detailed specification of the contact angle cell is given in earlier work by Hansen *et al.* [30]. The preparation methods for contact angle measurements were done following same procedure as reported earlier. In brief, pieces of the calcite crystals were filed using silicon carbide grinding paper ranging in grit size from coarse, P120, to the finest, P4000. After blowing off the loose calcite particles from the surface using air and washing with distilled water, they were dried at 120°C for 3 hours. The polished crystals were then pre-wetted in distilled water for 30 minutes. The water film on the surface is removed by air and the pre-wetted samples were immersed in 0.005M stearic acid (SA) dissolved in *n*-decane for 24 hours. The modified calcite was then rinsed by distilled water and *n*-heptane and dried under vacuum at ambient temperature (25°C) for 3 hours. At final stage, the modified calcite crystals were inserted inside the contact angle cell and advancing and receding contact angles of *n*-decane droplets in distilled water medium were measured. The measured contact angles reported here are within ±3°.

4.2.3. Reservoir Model Simulation

A simple 3D black oil (BO) model consisting of 1200 grid blocks (20x20x3) is used for the simulation done here, using the Eclipse reservoir simulator software version 2006a, provided by Schlumberger [17]. All input data such as reservoir geometric characteristics (e.g. porosity, absolute permeability, grid block size, etc.) and oil/water PVT data except relative permeability and temperature are kept constant. Other changes in input data are stated in the next section. The general reservoir model data are given in Table 6.

Table 6. Reservoir model input data.

Parameter	Amount
Porosity	$0.482^{(1)}$
Absolute permeability	$4.10^{(1)}$ md
Reservoir temperature	57.2°C (135°F)
Reservoir Fluids	Oil/water
Oil density	$0.7635^{(2)}$ (gr/cm^3)
Oil viscosity	$2.4826^{(2)}$ (cp)
Water density	$1.0016^{(2)}$ (gr/cm^3)
Water viscosity	$0.9913^{(2)}$ (cp)
No. of wells	2 (1 producer + 1 injector)

(1) From the work done by Hamouda *et al.* [16]

(2) Generated by PVTSim, version 17, 2007

Acknowledgements

References

1. Babadagli, T. Temperature effect on heavy oil recovery by imbibition in fractured reservoirs. *Journal of Petroleum Science and Engineering* **1996,** *14*, 197-208.
2. Babadagli, T. Evaluation of EOR methods for heavy oil recovery in naturally fractured reservoirs. *Journal of Petroleum Science and Engineering* **2003,** *37*, 25-37.
3. Babadagli, T.; Al-Bemani, A. Investigations on matrix recovery during steam injection into heavy-oil containing carbonate rocks. *Journal of Petroleum Science and Engineering* **2007,** *58*, 259-274.
4. Rao, D.N. Wettability Effects in Thermal Recovery Operations. *SPE Reservoir Evaluation and Engineering* **1999,** *2*, 420-430.
5. Tang, G.Q.; Morrow, N.R. Salinity, Temperature, Oil Composition and Oil Recovery by water flooding. *SPE Reservoir Engineering* **1997,** 269-276.

6. Tang, G.Q.; Morrow, N.R. Wettability Control by Adsorption from Crude Oil-Aspects of Temperature and Increases Water Saturation. Paper Presented in Int'l Symposium of Society of Core Analysts, Toronto, Canada, 21-25 August **2005**.

7. Al-Hadhrami, H.S.; Blunt, M.J. Thermally Induced Wettability Alteration To Improve Oil Recovery in Fractured Reservoirs. *SPE Reservoir Evaluation and Engineering* **2001,** *4* (3), 179-186.

8. Schembre, J.M.; Tang, G.Q.; Kovscek, A.R. Wettability alteration and oil recovery by water imbibition at elevated temperatures. *Journal of Petroleum Science and Engineering* **2006,** *52*, 131-148.

9. Hamouda, A.A.; Rezaei Gomari, K.A. Influence of Temperature on Wettability Alteration of Carbonate Reservoirs. Paper SPE 99848 presented at the Society of Petroleum Engineers/Department of Energy (SPE/DOE) Improved Oil Recovery Symposium, 22-26 April **2006,** Tulsa, OK.

10. Rezaei Gomari, K.A.; Karoussi, O.; Hamouda, A.A. Mechanistic Study of Interaction between Water and Carbonate Rocks for Enhancing Oil Recovery. Paper SPE 99628 presented at the Society of Petroleum Engineers (Europec/EAGE) Annual Conference and Exhibition, 12-15 June **2006,** Vienna, Austria.

11. Rezaei Gomari, K.A.; Hamouda, A.A.; Davidian, T.; Fagerland, D.A. In *Contact Angle, Wettability and Adhesion*; Mittal, K., Ed.; VSP: Leiden, The Netherland, 2006; Vol. 4, p.351.

12. Rezaei Gomari, K.A.; Hamouda, A.A. Effect of Fatty Acids, Water Composition and pH on the Wettability Alteration of Calcite Surface. Journal of Petroleum Science and Engineering **2006,** *50*, 140-150.

13. Rezaei Gomari, K.A.; Denoyel, R.; Hamouda, A.A. Wettability of Calcite and Mica Modified by Different Long Chain Fatty Acids (C18 Acids). *Journal of Colloid and Interface Science* **2006,** *297*, 470-479.

14. Karoussi, O.; Hamouda, A.A. Imbibition of Sulfate and Magnesium Ions into Carbonate Rocks at Elevated Temperatures and their Influence on Wettability. *Energy and Fuels* **2007,** *21*, 2138-2146.

15. Karoussi, O.; Hamouda, A.A. Macroscopic and nanoscale study of wettability alteration of oil-wet calcite surface in presence of magnesium and sulfate ions. *Journal of Colloid and Interface Science* **2008,** *317*, 26-34.

16. Hamouda, A.A.; Karoussi, O.; Chukwudeme, E.A. Relative permeability as a function of temperature, initial water saturation and flooding fluid compositions for modified oil-wet chalk. In review, *Journal of Petroleum Science and Engineering* **2008**.

17. Eclipse reservoir simulator reference manual, Schlumberger, **2006**.

18. Delshad, M.; Najafabadi, N.F.; Anderson, G.A.; Pope, G.A.; Sepehrnoori, K. Modelling Wettability Alteration in Naturally Fractured Reservoirs. Paper SPE 100081 presented at the Society of Petroleum Engineers/Department of Energy (SPE/DOE) Improved Oil Recovery Symposium, 22-26 April **2006,** Tulsa, OK.

19. Nakornthap, N.; Evans, R.D. Temperature-Dependant on Relative Permeability and Its Effect on Oil Displacement by Thermal Methods. *SPE Reservoir Engineering* **1986,** May, 230-242.

20. Schramm, L.L.; Manhardt, K.; Novosad, J. Electrokinetic properties of reservoir rock particles. *Colloids Surfaces A- Physicochemical and Engineering Aspects* **1991,** *55*, 309–331.

21. Pierre, A.; Lamarche, J. M.; Mercier, R.; Foissy, A.; Persello, J. Calcium as Potential Determining ion in Aqueous Calcite Suspensions. *Journal of Dispersion Science and Technology* **1990,** *11* (6), 611-635.

22. Amaefule, J.O.; Handy, L.L. The Effect of Interfacial Tension on Relative Oil/Water Permeabilities of Consolidated Porous Media. *SPE Journal* **1982,** 371-381.

23. Kumar, S.; Torabzadeh, S.J.; Handy, L.L. Relative Permeability Function for High- and Low-Tension Systems at Elevated Temperatures. Paper SPE 13670 presented at the Society of Petroleum Engineers California Regional Meeting, 27-29 March **1985,** Bakersfield, CA.

24. Bahramian, A.; Danesh, A. Prediction of solid–water–hydrocarbon contact angle. *Journal of Colloid and Interface Science* **2007,** *311*, 579-586.   .

25. Cassé, F.J.; Ramey, H.J. Jr. The Effect of Temperature and Confining Pressure on Single-Phase Flow in Consolidated Rocks. *Journal of Petroleum Technology* **1979,** *31* (8), 1051-1059.

26. Weinbrandt, R.M.; Ramey, H.J. Jr.; Cassé, F.J. The Effect of Temperature on Relative and Absolute Permeability of Sandstones. *SPE Journal* **1975,** *15* (15), 379-384.

27. Gray, D.H.; Fatt, I.; Bergamini, G. The Effect of Stress on Permeability of Sandstone Cores. *SPE Journal* **1963,** *3* (2), 95-100.

28. Sedaee Sola, B.; Rashidi, F.; Babadagli, T. Temperature effects on the heavy oil/water relative permeabilities of carbonate rocks. *Journal of Petroleum Science and Engineering* **2007,** *59*, 27-42.

29. Lee, A.L.; Ellington, R.T. Viscosity of n-Decane in the Liquid Phase. *Journal of Chemical Engineering and Data* **1965,** *10* (4), 346-348.

30. Hansen, G.; Hamouda, A. A.; Denoyel, R. The Effect of Pressure on Contact Angles and Wettability in the Mica/Water/n-decane System and the Calcite+stearic acid/water/n-decane System. *Colloids Surfaces A- Physicochemical and Engineering Aspects* **2000,** *172*, 7-16.